Available online at www.sciencedirect.com
ScienceDirect
Polymer 48 (2007) 338–347
polymer
www.elsevier.com/locate/polymer

Studies on the formation of self-assembled nano/microstructured polyaniline–clay nanocomposite (PANICN) using 3-pentadecyl phenyl phosphoric acid (PDPPA) as a novel intercalating agent cum dopant

J.D. Sudha*, T.S. Sasikala

Chemical Sciences Division, Polymer Section, Regional Research Laboratory (CSIR), Thiruvananthapuram 695019, Kerala, India

Received 28 August 2006; received in revised form 17 October 2006; accepted 25 October 2006
Available online 20 November 2006

Abstract

Novel self-assembled micro/nanostructured polyaniline–clay nanocomposite (PANICN) materials were prepared by *in situ* intercalative emulsion polymerization of aniline in aqueous dispersion of clay using functionalized amphiphilic dopant, 3-pentadecyl phenyl phosphoric acid (PDPPA) derived from renewable resource. The structural effect of PDPPA on the morphology, electrical conductivity and phase transition temperature of PANICNs was compared with nanocomposites prepared using dodecyl benzene sulphonic acid (DBSA) and HCl. X-ray diffraction and scanning electron microscopic (SEM) studies revealed the formation of monolayer of protonated PANI intercalated nanoclay layers with template polymerized self-assembled micro/nanostructured PANI on the surface of the clay. Nano/microstructured PANIs were formed by the supra-molecular self-assembling of the inter-chain hydrogen bonding, interplane phenyl stacking and electrostatic layer-by-layer self-assembling (ELBS) between polarised alkyl chains present in dopant anions and were manifested using Fourier transform infrared spectroscopy and differential scanning calorimetry.

Keywords: Polyaniline; Intercalative polymerization; Nanostructured

1. Introduction

In recent years, electrically conducting polyaniline–clay nanostructured (PANICNs) materials including nanofibers and nanotubes have been prepared by different strategies for potential applications [1]. Mechanical, thermal and environmental stabilities are desired for electrically conducting PANI in advanced electronic and optical applications including rechargeable batteries, energy storage, electromagnetic interference shielding and chemical sensing devices. Synthesis of polyaniline–clay hybrid/nanocomposite (PANICN) is receiving attention in this respect due to better conductivity and more economical efficiency with low loading of PANI [2,3].

There are many routes for preparing these materials, through micellar media [4], interfacial [5], template-guided [6] or aniline polymerization in the presence of inorganic or organic matrices resulting in PANI composites [7–9]. Among these synthetic approaches, the formation of PANI nanocomposites has received great attention, since it is possible to use this method to get PANI with ordered chain structure and with better properties than that of bulk ones. The most common inorganic matrix used to prepare PANI composites is smectite clay [8,9], due to its capacity to swell and exchange cations. Bentonite is a naturally occurring inexpensive layered silicate which organize themselves in a parallel fashion to form stacks with a regular van der Waals gap in-between them called interlayer spacing and the galleries contain metal cations (Na^{1+}, Li^{1+}, Ca^{2+}), which are exchangeable with organic cations [10]. The functionalized intercalating cum dopant can act as a surfactant for reducing the intergallery interaction and will promote the

* Corresponding author. Tel.: +91 471 2515316; fax: +91 471 2491712.
E-mail address: sudhajd2001@yahoo.co.in (J.D. Sudha).

0032-3861/$ - see front matter © 2006 Elsevier Ltd. All rights reserved.
doi:10.1016/j.polymer.2006.10.030

expansion of intergallery due to the presence of both hydrophobic and hydrophilic group. The commonly used dopants for PANI are mineral acids and amphiphilic molecules such as sulphonic acids [11], phosphonic acids [12] and phosphoric acid esters [13]. Herein we report the use of a few molecular systems derived from 3-pentadecyl phenol (3-PDP) which is obtained from renewable resource material, cashew nut shell liquid [14]. The presence of both hydrophobic (alkyl) and hydrophilic ($-SO_3H/-HPO_4$) groups enables it to function as an intercalating agent as well as dopant similar to DBSA. After intercalation of the anilinium ion (An^+) ^-OR, the extrinsic initiator ammonium persulphate (APS) can enter and initiate polymerization for getting protonated PANI chain confined PANICNs. Structurally, two kinds of clay polymer nanocomposites can be isolated: (i) intercalated nanocomposites where polymer chains are between the clay layers and a regular repeating distance can be observed; (ii) exfoliated nanocomposite where clay stacks are delaminated forming individual layers dispersed within the polymer. When aniline polymerization is done in an acidic aqueous suspension of bentonite having one oxidizing agent, the formation of intercalated and/or exfoliated nanocomposite can be dependent on aniline to intercalating agent ratio. Kim et al. [15] have prepared polyaniline–clay nanocomposite (PANICN) by *in situ* intercalative emulsion polymerization using DBSA as intercalating agent cum functionalized dopant. Mesomorphic behavior of hydrogen-bonded self-assembled complexes of methyl sulphonic acid (MSA), polyvinyl pyridine (PVP) and 3-PDP, which is the starting material for the preparation of PDPPA, was reported by Ikkala and ten Brinke [16]. They reported that self-assembled nanostructures were formed through hydrogen bonding and also by electrostatic layer-by-layer self-assembling (ELBS) between the polarised hydrocarbon chains present in PDP.

In the present work, we report the studies on the synthesis and properties of micro/nanostructured protonated PANICNs using 3-PDPPA as intercalating agent cum dopant which is a bifunctional molecule having long alkyl chain *meta* to the $-H_2PO_4$ group and is derived from renewable resource and the properties were compared with DBSA, which is built with alkyl chain *para* to the sulphonic acid group. Effect of compositional variation of aniline/dopant/clay on the morphology and other physical properties of PANICNs were discussed.

2. Experimental section

2.1. Materials

Aniline monomer (99.5% purity, Ranbaxy Chemicals Ltd., Bombay) was distilled under reduced pressure, anilinium hydrochloride, ammonium persulphate (APS), methyl alcohol (SD Fine Chemicals Limited, Bombay). Bentonite clay with cation exchange capacity of 55 meq/100 g and a mean chemical formula of $(Na,Ca)_{0.33}(Al_{1.67}Mg_{0.33})Si_4O_{10}(OH)2nH_2O$ (Loba Chemie, Bombay, India) was used. Prior to use, it was washed with saturated sodium chloride solution many times and size fractionated to obtain Na–bentonite free of impurities. DBSA (85% purity, Aldrich, Germany) PDPPA was prepared from cardanol obtained by the double distillation of cashew nut shell liquid (Cashew Export Promotion Council, India) at 3–4 mm Hg at 230–235 °C. This was hydrogenated to 3-pentadecyl phenol as per the procedure in Ref. [13].

2.2. Preparation of 3-pentadecyl phenyl phosphoric acid (PDPPA)

3-Pentadecyl phenol (0.8 mol) 60 ml and dry hexane 600 ml were taken in a round-bottomed flask. To the stirring solution phosphorous pentoxide (0.13 mol) 18 g was added in portion wise. The reaction was continued for 6 h at 80–85 °C. The pyrophosphate formed was hydrolysed with dil. HCl. Then it is filtered and dried under vacuum at 80 °C for 6 h.

Formation of PDPPA was confirmed by elemental analysis, FTIR and ^1H NMR spectra. Elemental analysis calculated for molecular formula $C_{21}H_{38}PO_4$: %C = 65.4; %H = 9.8; %P = 8.0; observed: %C = 65.1; %H = 9.6; %P = 7.9. In FTIR spectra, the ν (max) 2919, 2841, 1469 $(-CH_2-)_n$, 1605, 694 (Ar), 1227 (CO), 1250 (P=O), 2730 (P–OH), 3020 (C–H), 2980 (aliphatic). ^1H NMR ($CDCl_3$, ppm): δ 0.8–0.9 (3H, t, CH_2-CH_3), 1.25 (26H, br s, $(-CH_2-)_n$, 2.8 (2H, t, $(Ph-CH_2-)_n$, 5.7 (1H, br s, OH), 6.8–6.9 (3H, m, Ar), 7.0 (1H, d, ArC-5) (Scheme 1).

2.3. Preparation of polyanilines (PANIs) and polyaniline–clay nanocomposites (PANICNs)

PANICN with different molar ratios of dopant was prepared by an *in situ* intercalative emulsion polymerization method. Bentonite 2.5 g was dispersed in 200 ml deionised water by heating and stirring at 80 °C for 3 h. Aniline 2.3 g (0.025 mol) was mixed with PDPPA 90 g (0.025 mol) and dispersed in water/xylene mixture. This emulsion was then added drop-wise to clay dispersion. Then it was heated with stirring for 6 h at 100 °C. The mixture was cooled down to 0 °C by keeping in an ice bath and the pH was regulated to 2 with HCl. The oxidant initiator $(NH_4)_2S_2O_8$ (0.03 mol) dissolved in 50 ml of distilled water was then added drop-wise to initiate the polymerization. Reaction continued for 10 h. The dark green color precipitate was isolated by adding methanol, filtered, washed with deionised water and dried at 60 °C in a vacuum oven by keeping for 16 h. Experiments were performed with different ratios

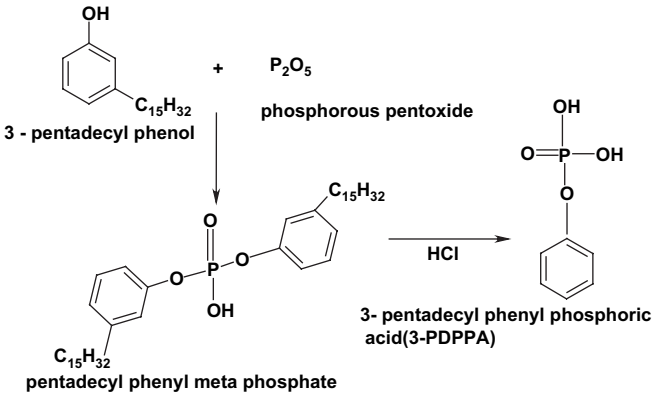

Scheme 1. Synthesis of PDPPA.

of aniline/PDPPA. PANICNs prepared using DBSA, PDPPA, HCl are indexed as PANICN–DBSA, PANICN–PDPPA and PANICN–HCl, respectively.

PANI–DBSA, PANI–PDPPA and PANI–HCl were also prepared without clay for comparison.

2.4. Characterization techniques

2.4.1. Measurement of UV–vis spectra

UV–vis spectra of the PANICN samples were obtained from Perkin–Elmer in a wavelength range of 300–1000 nm.

2.4.2. Measurement of FTIR and NMR spectra

PANIs and PANICNs were dispersed in potassium bromide and compressed into pellets to record FTIR spectrum. The measurements were made with a fully computerized Nicolet Impact 400D FTIR spectrophotometer. All spectra were corrected for the presence of moisture and carbon dioxide in the optical path. ^{1}H NMR spectra were recorded with $CDCl_3$ using Brucker 300 MHz FT-NMR equipped with ASPECT-3000 computer.

2.4.3. X-ray diffraction (XRD) measurements

X-ray diffraction (XRD) measurements were carried out using a Philips X-ray diffractometer using nickel filtered Cu Kα radiation ($\lambda \sim 0.154$ nm). Powder form was used for the XRD experiments. Patterns were recorded in the 2θ angles from 2 to 40°.

2.4.4. Electrical conductivity

PANIs and PANICNs were compressed with a manual hydraulic press at 800 MPa into pellets with 50 mm diameter and 1 mm thick. The conductivity was measured by a standard spring loaded pressure contact four-probe method supplied by Scientific Equipment, Roorkee (India). The conductivity (σ_0) was calculated using van der Pauw relation

$$\sigma_0 = (\ln 2/\pi d)(I/V),$$

where d is the thickness of the film.

2.4.5. Measurement of scanning electron microscopy

Morphological studies of PANICN powder samples were examined using scanning electron microscope (SEM, JEOL make, model JSM 5600 LV) at 15 kV accelerating voltage.

2.4.6. Differential scanning calorimetry

DSC measurements were made with Dupont DSC 2010 differential scanning calorimeter attached to Thermal Analyst 2100 at a heating rate of 10 °C/min in nitrogen atmosphere.

3. Results and discussion

3.1. Preparation of polyanilines (PANIs) and polyaniline–clay nanocomposites (PANICNs)

PDPPA was found to act as intercalating agent cum dopant for the preparation of PANICN–PDPPAs as shown in Scheme 2 [15]. Experiments were performed with and without the presence of clay and also with different ratios of aniline to dopant (PDPPA and DBSA). The induction period and polymerization time were recorded from the beginning of the oxidant addition to the reaction mixture until the color turned pale blue and dark green, respectively. Details of induction period, yield and polymerization time are summarized in Table 1. The induction period for PANI–PDPPA (140 min) is higher than PANICN–DBSA (15–25 min). This might be due to less degree of absorption of the An^+ PDPPA complex on the clay layers. After the insertion of An^+ into the galleries, a coordinate bond is formed between the monomer and the ions present in the silicate gallery. The polymer chain can add monomer until its oxidation stage achieves emeraldine green form. At this point, oxidation potential becomes very slow and polymerization stops.

UV–vis reflectance spectra of the PANICN–PDPPA, PANICN–HCl, PANICN–DBSA, PANI–PDPPA, PANI–DBSA, PANI–HCl are shown in Fig. 1a–f, respectively. PANI–HCl, PANI–PDPPA and PANI–DBSA exhibited two broad absorption maxima in the range of 300–440 nm and 520–700 nm. The absorption peak in the 340 nm is assigned as the π–π^* transition in the reduced unit of polyaniline as reported in the literature [17]. The absorption band at 700 nm is characteristic of the head to tail coupling of anilinium radical cations of the PANI–ES [18]. In PANICN–HCl, PANICN–PDPPA and PANICN–DBSA, a red shift in the second maximum is observed as a broad absorption band (called ''free carrier tail'') in the near infrared region [19]. It is consistent with the delocalization of electrons in the polaron band promoted by an extended confirmation of the polymer chain inside the nanoclay layers.

FTIR spectra of the PANI–HCl, PANICN–HCl, PANI–PDPPA, PANICN–DBSA, PANI–DBSA, PANICN–PDPPA, bentonite are shown in Fig. 2a–g, respectively. The characteristic bands corresponding to bentonite (Fig. 2g) appeared at 1023 [ν (Si–O)], 911 [δ (Al–OH)] and 525 cm^{-1} (ν (Si–O–Al)] [20]. PANI–PDPPA (Fig. 2c) presented four major vibration bands at 1116 [*para*-substituted aromatic δ (C–H) in plane], 1295 [ν (C–N), 1487 [benzenoid ring ν (C=C)] and 1560 cm^{-1} [quinoid ring ν (C=C)] and these observed bands are in good agreement with the previously published values [21]. The P=O stretching mode occurring at 1248 cm^{-1} is superimposed on B–B–B stretching of PANI occurring at 1238 cm^{-1}. The band at 1295 cm^{-1} for the PANI–HCl, PANICN–HCl, PANI–PDPPA, and PANI–DBSA (Fig. 2a–c, and e, respectively) assigned as the stretching vibration of C–N [ν (C–N)], is significantly shifted to 1303 cm^{-1} for the intercalated nanocomposites of PANICN–PDPPA and PANICN–DBSA as shown in Fig. 2f and d, respectively. Consequently, the frequency shift of ν (C–N) observed in PANICNs is believed to be caused by the hydrogen-bonded interaction between PANI and the basal surface of nanoclay (*i.e.* NH···O hydrogen bonding). The absorption bands around 3423 cm^{-1} and 3230 cm^{-1} and 2300–2800 cm^{-1}, reflect the organization of PANI chains by hydrogen-bonded interaction involving NH and NH^+ groups [22].

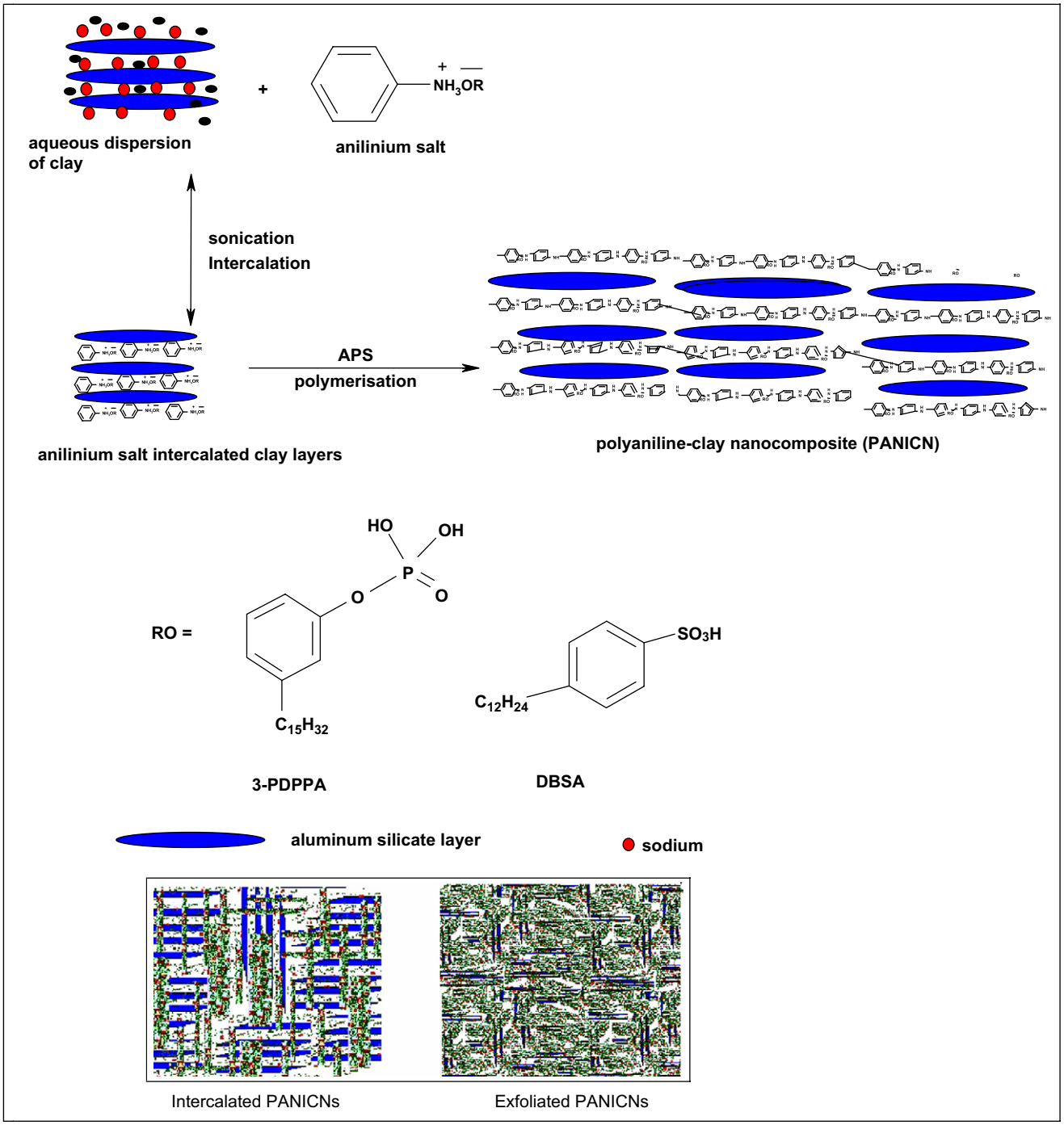

Scheme 2. Synthesis of PANICNs.

3.2. XRD measurements

During intercalation, the PANI–dopant chains get confined in the inter-clay layers; the inter-distance between the clay layers increases in various directions depending on the conformation and functionality of the intercalating chains. We estimate the variation of d-spacing, which is induced from the angular position 2θ of the observed peaks according to the Bragg formula $n\lambda = 2d \sin\theta$. The XRD patterns of bentonite, PANICN–HCl, PANI–HCl, PANI–PDPPA, PANICN–PDPPA3, PANICN–DBSA1, PANICN–DBSA3, PANICN–PDPPA1, PANI–DBSA are shown in Fig. 3a–i. The XRD pattern of bentonite (Fig. 3a) at low angle exhibited a sharp peak at $2\theta = 6.4°$ (13.6 Å) corresponding to interlayer spacing of the aluminum silicate layer. The diffraction pattern of PANI–HCl appeared as featureless whereas the PANI–PDPPA (Fig. 3d) and PANI–DBSA (Fig. 3i) exhibited diffractogram with specific features. Diffractogram of PANI–PDPPA appeared as a sharp peak at $2\theta = 3.1$ with d-spacing of 30 Å which corresponds to the electrostatic layer-by-layer self-assembly of

Table 1
Experimental details of the preparation of PANI–PDPPA, PANICN–PDPPA, PANI–DBSA and PANICN–DBSA

Sample	Ratio of aniline:dopant	Temperature of intercalation (°C)	Induction period (min)	Polymerization time (h)	Yield (%)	Color and appearance
PANI–PDPPA	1:1	NA	140	8	75	E.G. fine powder
PANICN–PDPPA1	1:0.5	120	100	8	55	E.G. fine powder
PANICN–PDPPA2	1:1	120	80	8	69	E.G. fine powder
PANICN–PDPPA3	1:1.5	120	60	10	70	E.G. fine powder
PANICN–PDPPA4	1:2	120	40	16	78	E.G. fine powder
PANI–DBSA	1:1	NA	40	8	74	E.G. fine powder
PANICN–DBSA1	1:0.5	80	25	8	60	E.G. fine powder
PANICN–DBSA2	1:1	80	20	8	78	E.G. fine powder
PANICN–DBSA3	1:1.5	80	18	10	65	E.G. fine powder
PANICN–DBSA4	1:2	80	15	18	72	E.G. fine powder

E.G. = emeraldine green.

protonated PANI–DBSA (Table 2) as observed by Taka et al. [23] (Scheme 3). PANICN–PDPPA1 (Fig. 3h) exhibited two reflections below $2\theta = 10°$, the broad diffractograms at $2\theta = 5.8°$ and 3.3° with a *d*-spacing of 16.7 Å and 33 Å. Taking into account the clay thickness as 9.6 Å, the basal spacing of 16.7 Å corresponds to the gallery height of 7 Å. The initial enhancement in the interlayer spacing is very close to the dimension of polyaniline which is similar to that reported for V_2O_5 [24] and FeOCl [25]. Second peak observed is due to the layered arrangement of PANI–PDPPA engulfed over the clay surface. Diffractogram of PANICN–DBSA1 (Fig. 3f) exhibited two maxima with a *d*-spacing of 16.4 Å and 38 Å. The initial peak is due to the enhancement in the interlayer spacing (6.8 Å) associated with the confinement of the PANI chains and the other reflection is due to the layered arrangement of the protonated PANI–DBSA. Fig. 3e and g represents the diffractogram of PANICN–PDPPA3 and PANICN–DBSA3 having aniline to intercalating agent ratio of 1:1.5. Diffractogram exhibited peak that corresponds to the self-assembled layered structure of protonated PANIs without the d_{001} reflection. This can be due to the exfoliated structure of PANICNs. Diffractogram of PANI–DBSA (Fig. 3i) corresponds to the self-assembled layered structure of PANI–DBSAs. In the case of PANICN–HCl, the peak is shifted to lower angle ($2\theta = 6.3°$) with *d*-spacing of 13.9 Å. The enhancement in the interlayer spacing is smaller than the dimension of the PANI chains which showed the non-confinement of PANI chains between the clay layers. It was also observed that

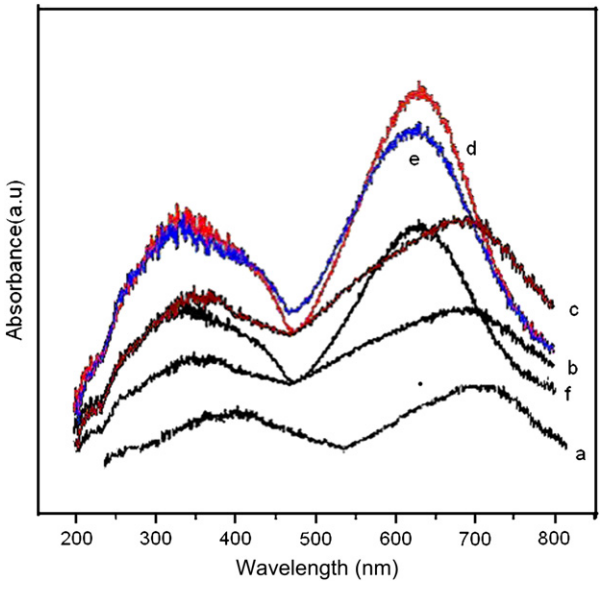

Fig. 1. UV–Vis spectra of (a) PANICN–PDPPA, (b) PANICN–HCl, (c) PANICN–DBSA1, (d) PANI–PDPPA, (e) PANI–DBSA, and (f) PANI–HCl.

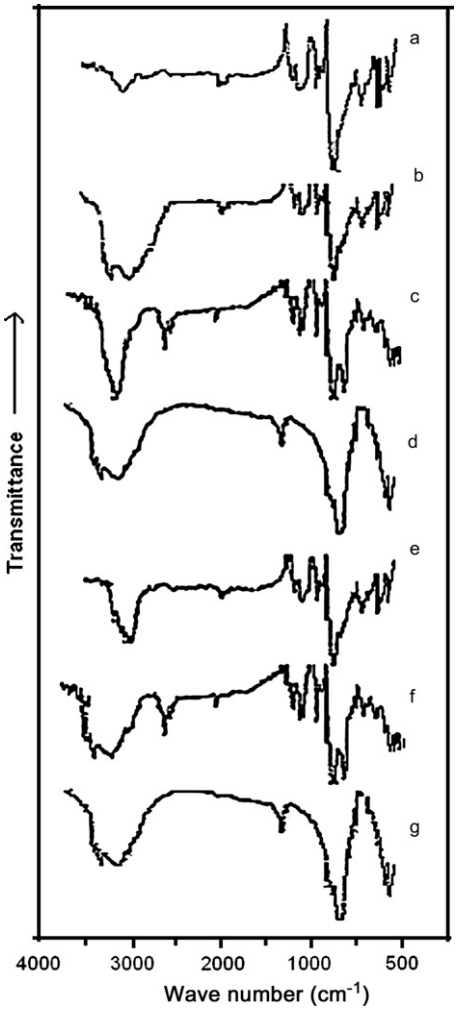

Fig. 2. FTIR spectra of (a) PANI–HCl, (b) PANICN–HCl, (c) PANI–PDPPA, (d) PANICN–DBSA, (e) PANI–DBSA, (f) PANICN–PDPPA, and (g) bentonite.

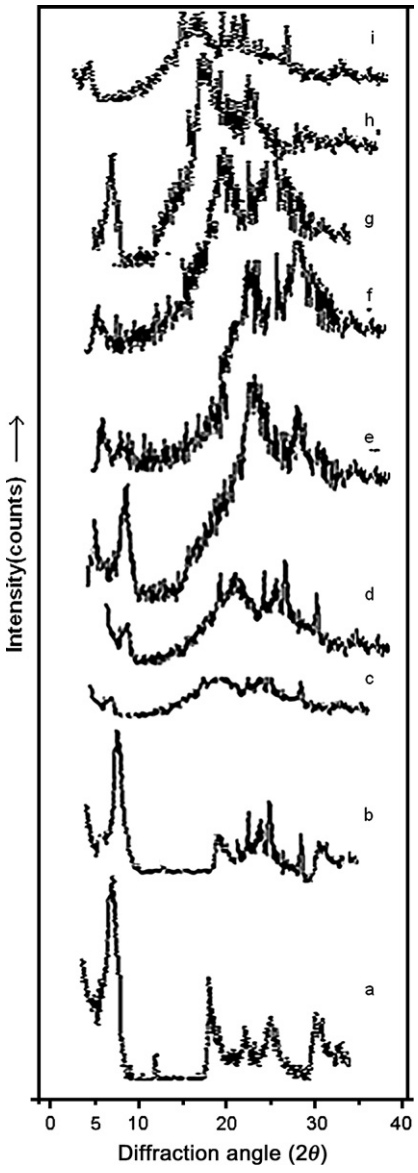

Fig. 3. Small angle XRD of (a) bentonite, (b) PANICN–HCl, (c) PANI–HCl, (d) PANI–PDPPA, (e) PANICN–PDPPA3, (f) PANICN–DBSA1, (g) PANICN–DBSA3, (h) PANICN–PDPPA1, and (i) PANI–DBSA.

in PANICN–DBSA and PANICN–PDPPA, the characteristic d_{004}-spacing at $2\theta = 20^\circ$ of the bentonite is also distorted due to intercalation/exfoliation (Table 2).

Table 2
Experimental details of SAXD analysis

System	*d*-spacing (Å)	Angle 2θ (°)
Bentonite	13.6	6.4
PANI–HCl	No peak	No peak
PANICN–HCl	13.9 (broad)	6.3
PANI–PDPPA	30 (broad)	3
PANICN–PDPPA1	34 (weak), 16.7 (strong)	3.3, 5.8
PANICN–PDPPA2	42.2 (strong), 16.9 (weak)	2.0, 5.7
PANICN–PDPPA3	Featureless	No peaks
PANI–DBSA	28 (sharp)	3.1
PANICN–DBSA1	38, 14.7 (broad)	2.29, 5.96
PANICN–DBSA2	40 (sharp), 16.7 (broad)	2.1, 5.8
PANICN–DBSA3	43.1 (sharp), 16.41 (weak)	2.04, 5.96

3.3. Electrical conductivity measurements

The dc conductivity (σ_{dc}) measurements of PANICNs were carried out using four-probe conductivity meter with uniform sized pellets. The conductivity was found to depend on the structure and molar ratio of the dopants. Conductivity measurements were carried out as a function of increasing amount of dopant by keeping clay to aniline ratio constant and the data are shown in Table 3. Increasing the amount of dopant increases the degree of protonation. That is why increased degree of protonation on the imine nitrogens leads to a higher conductivity. The classical protonation (doping) concept assumes that the acid reacts with the imine nitrogens in PANI (emeraldine) base and as a result PANI 'salt' is produced. The two electrons from the electron pairs located at imine nitrogens are injected into the adjacent quininoid ring, which is converted to the benzenoid form. The remaining unpaired electron present in the imine nitrogens and cation radicals act as carriers in the electric conduction. PANI–PDPPA showed conductivity of 8.2×10^{-1} S/cm (1:1). PANICN–PDPPA exhibited conductivity values 1.28×10^{-4}, 1.28×10^{-3}, 8.8×10^{-3}, 7.2×10^{-2} S/cm for different aniline/PDPPA molar ratios, 1:0.5, 1:0.75, 1:1, 1:1.5, respectively. The conductivity values of PANI–HCl and PANICN–HCl are measured as 3.6×10^{-4} and 2.85×10^{-4} S/cm, respectively.

Conductivity values of PANI–DBSA and PANICN–DBSA decreased when the ratio of [aniline]:[DBSA] is varied from 1:0.5 to 1:2. The low value of conductivity for the PANI–PDPPA systems compared to DBSA is due to the bulky and divalent nature of the PDPAA [26].

3.4. SEM measurements

The SEM micrographs of bentonite, PANI–PDPPA, PANI–DBSA, PANICN–PDPPA1, PANICN–PDPPA2, PANICN–PDPPA3, PANICN–DBSA3 are shown in Fig. 4a–g, respectively. The morphology of bentonite was observed as flaky texture reflecting its layered texture as shown in Fig. 4a [27]. It was observed that the microstructure of PANICNs is highly dependent on the quantity and the nature of the dopant. The microstructure of PANI–PDPPA (Fig. 4b) was observed as cylindrical shaped aggregates with uniform distance between protonated PANI chains. The thickness of the aggregate was observed as 30 Å in the XRD measurements. The micrograph of PANI–DBSA (Fig. 4c) is observed as lamellar shaped structures with thickness of 32 Å and is uniformly distributed compared with PANI–PDPPA. Fig. 4d–f represents the micrographs of PANICN–PDPPAs with molar ratio of [aniline]:[dopant] 1:0.5, 1:0.75, 1:1.5, respectively. Fig. 4d represents PANICN–PDPPA1 having PANI chain intercalated sheets with the less number of sheets. PANICN–PDPPA2 (Fig. 4e) observed as clay sheets engulfed with sheets and also some PANI chain engulfed sheets. Fig. 4f shows the fully exfoliated clay layers engulfed with the formation of template polymerized self-assembled PANI chains. Fig. 4g is the micrograph observed for PANICN–DBSA3 for 1:1.5 aniline to DBSA molar ratio which showed a bunch of

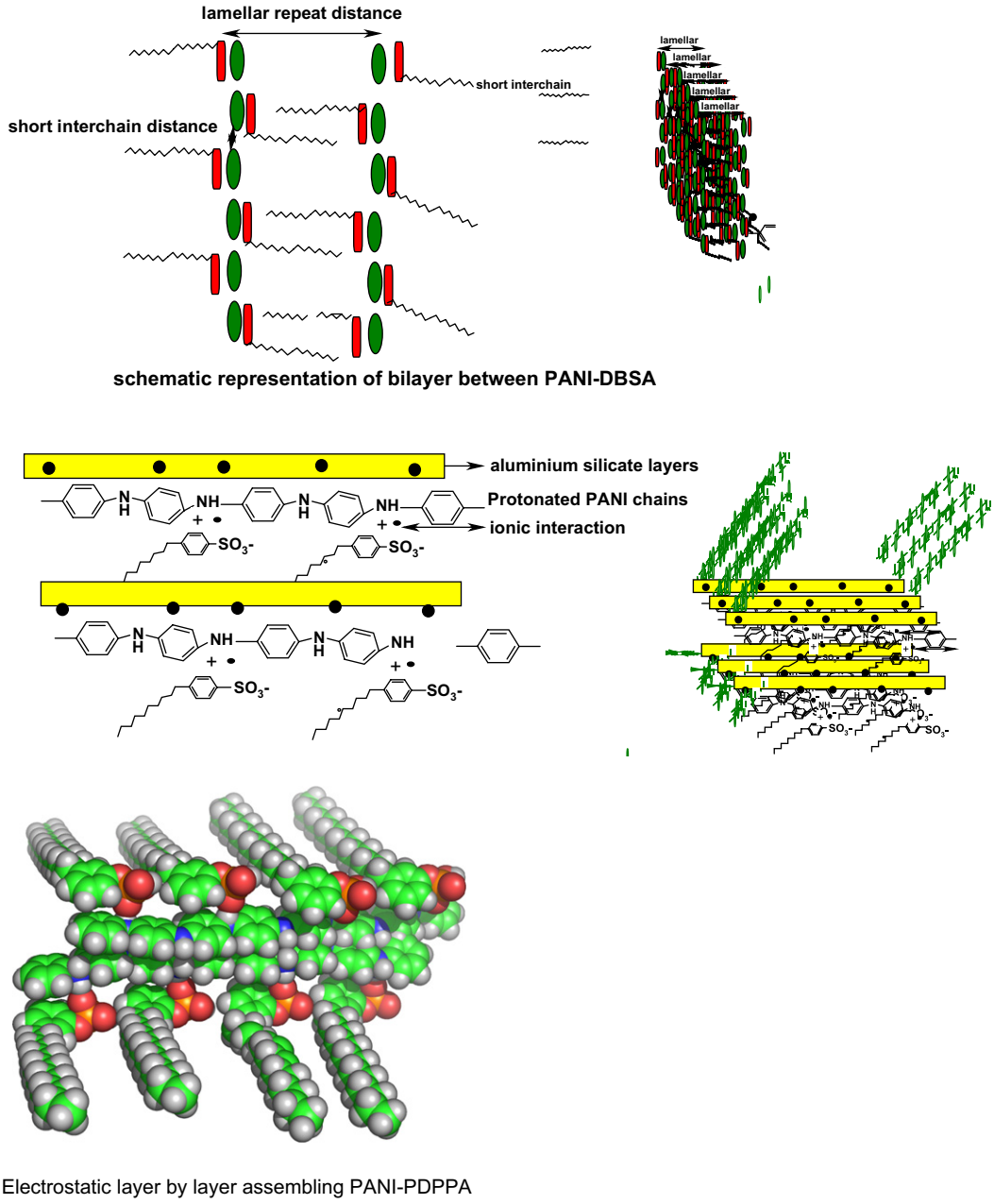

Scheme 3. Schematic representation of self-assembling in PANI–DBSA, PANI–PDPPA in PANICNs.

micro/nanometer-sized filaments in comb shaped structure. The micelle formed by the hydrophilic aniline with the hydrophobic amphiphilic surfactant will play a role in forming templates on the clay surface that facilitate the formation of nano/microstructures of PANICN–PDPPA. It was also observed that colorless round shaped micelles formed on the surface of the rods (Fig. 4e and f). These sprouts might have been formed by the self-assembled anilinium phosphate salts by ELBS which may be acting as template for the formation of nanostructure rods as shown in Scheme 2. Thus, it is clear that the morphology of PANIs and PANICNs was controlled by the structure and amount of the amphiphilic dopant. Based on the above observations, a schematic representation for the

Table 3
Details of the conductivity measurement of PANI and PANICNs

System	Conductivity (S/cm)
PANI–PDPPA	8.2×10^{-1}
PANICN–PDPPA1	1.28×10^{-4}
PANICN–PDPPA2	1.28×10^{-3}
PANICN–PDPPA3	8.8×10^{-3}
PANICN–PDPPA4	7.2×10^{-2}
PANI–DBSA	3.0
PANICN–DBSA1	3.2×10^{-3}
PANICN–DBSA2	8.8×10^{-2}
PANICN–DBSA3	2.2×10^{-1}
PANICN–DBSA4	7.1×10^{-1}
PANI–HCl	3.6×10^{-4}
PANICN–HCl	2.85×10^{-4}

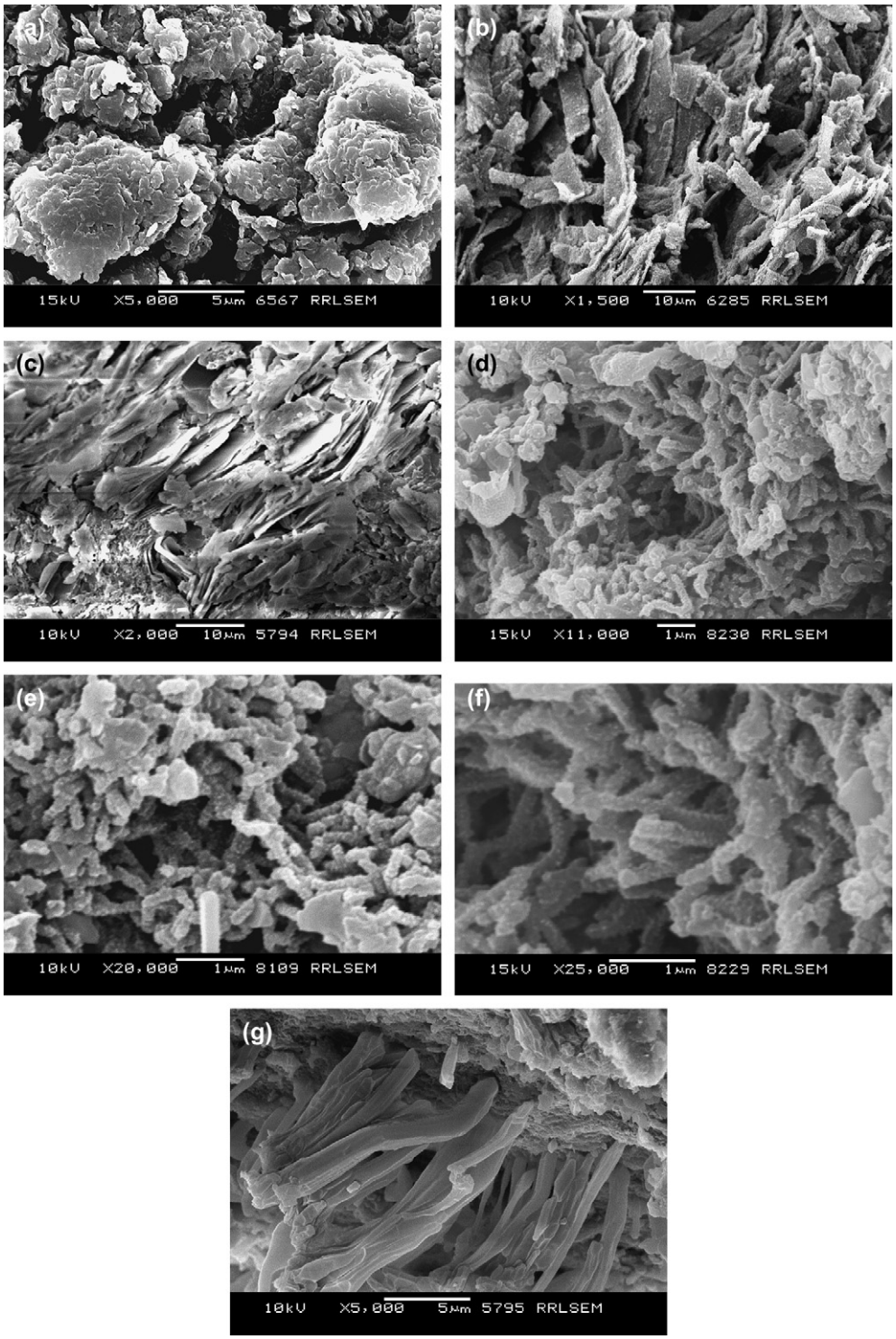

Fig. 4. SEM pictures of (a) bentonite, (b) PANI–PDPPA, (c) PANI–DBSA, (d) PANICN–PDPPA1, (e) PANICN–PDPPA2, (f) PANICN–PDPPA3, and (g) PANICN–DBSA3.

formation of PANICN nanostructures was proposed as shown in Scheme 2.

3.5. Differential scanning calorimetry

Thermal phase transition changes of PANIs and PANICNs were studied by DSC at a heating rate of 10 °C/min under nitrogen atmosphere. The DSC curves of PANICN–DBSA2, PANICN–PDPPA2, PANICN–HCl, PANI–PDPPA, PANI–DBSA, and PANI–HCl are shown in Fig. 5a–e, respectively. DSC curves of PANI–HCl and PANICN–HCl did not exhibit any thermal phase transition change up to 250 °C. PANI–PDPPA and PANI–DBSA showed endothermic phase transition around 75 and 95 °C, respectively.

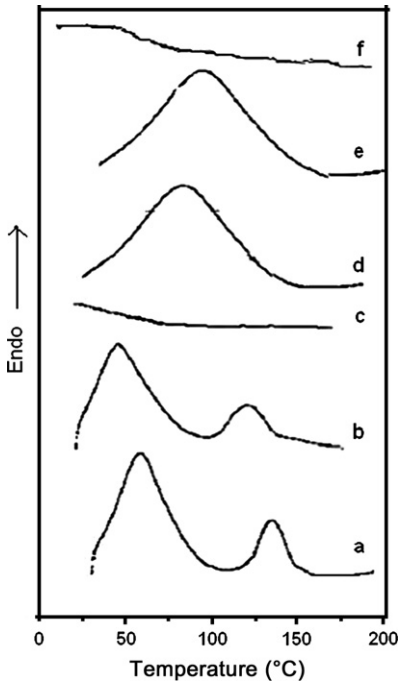

Fig. 5. DSC curves of (a) PANICN–DBSA2, (b) PANICN–PDPPA2, (c) PANICN–HCl, (d) PANI–PDPPA, (e) PANI–DBSA, and (f) PANI–HCl.

This energy change is arising due to the conformational change of the hydrogen-bonded protonated PANI–PANI chains as explained by Ikkala and ten Brinke [28]. On heating, PANICNs undergo change in energy that can arise from two factors. DSC scan of PANICN–PDPPA2 and PANICN–DBSA2 exhibited two endotherms. The first endotherm is observed around 50 °C for PANICN–PDPPA2 and that for PANICN–DBSA2 is observed at 55 °C due to the conformational change of the hydrogen-bonded protonated PANI–PANI chains. Second transition takes place around 135 and 148 °C for PANICN–PDPPA2 and PANICN–DBSA2, respectively, due to the interaction of the PANI chains and the clay layer as observed in PANI chain confined layered materials [29].

4. Conclusion

In conclusion PDPPA derived from renewable resource is a low cost intercalating agent cum dopant which can be successfully used for the preparation of micro/nanostructured polyaniline–clay nanocomposite similar to DBSA. Thus the unique structure of the PDPPA plays a dual role of intercalating agent cum dopant. Nanocomposites containing both intercalated and exfoliated PANICNs were prepared by changing the molar ratio of aniline and intercalating agent. The prospects for the direct application of these nanocomposites can be used in mitigating electric charge since these composites are easily dispersible with other polymers for making blends. Future work will emphasize on decreasing tube size for increasing the dispersability and conductivity.

Acknowledgements

We are grateful to Council of Scientific and Industrial Research (CSIR, India) for financial support (Task force fund COR 004). We are also thankful to Mr. P. Prabhakar Rao for all the useful discussions and SEM pictures, P. Guruswamy for all the X-ray diffractograms and P. Mukundan for FTIR spectra.

References

[1] (a) Kanatzidis MG, Wu CG, Marcy HO, Kannewurf CR. J Am Chem Soc 1989;111:4139;
(b) Cox SD, Stucky GD. J Phys Chem 1991;95:710;
(c) Enzeland P, Bein T. J Phys Chem 1989;93:6270.
[2] (a) Enzel P, Bein T. Chem Mater 1992;4:819;
(b) Pillion JE, Thompson ME. Chem Mater 1991;3:777;
(c) Nazar LF, Zhang Z, Zinkweg D. J Am Chem Soc 1992;114:6239;
(d) Ruiz-Hitzky E. Adv Mater 1993;5:334.
[3] Qui H, Wan M, Mathews B, Dai L. Macromolecules 2001;34:675.
[4] (a) Han MG, Cho SK, Oh SG, Im SS. Synth Met 2002;126:53;
(b) Wei Z, Zhang Z, Wan M. Langmuir 2002;18:917;
(c) Guo X, Luo K, Shi N. J Mater Sci Technol 2005;21:179.
[5] (a) Huang J, Kaner RB. J Am Chem Soc 2004;126:851;
(b) Huang J, Kaner RB. Angew Chem Int Ed 2004;43:5817;
(c) Tan KL, Tan BTG, Kang ET, Neoh KG. Phys Rev B 1989;39:8070.
[6] (a) Martin CR. Acc Chem Res 1995;28:61;
(b) Hulteen JC, Martin CR. J Mater Chem 1997;7:1075;
(c) Martin CR. Science 1994;26:1961.
[7] (a) Wu Q, Xue Z, Qi Z, Hung F. Polymer 2000;41:2029;
(b) Wu Q, Xue Z, Qi Z, Wang F. Acta Polym Sin 1999;5:551.
[8] (a) Chang TC, Ho SY, Chao KJ. J Chin Chem Soc 1992;39:209;
(b) Feng B, Su Y, Song J, Kong K. J Mater Sci Lett 2001;20:293;
(c) Inoue H, Yoneyama H. J Electroanal Chem 1987;233:291.
[9] (a) Frisch HL, Xi B, Qin Y, Rafailovich M, Yang NL, Yan X. High Perform Polym 2000;12:543;
(b) Biswas M, Ray SS. J Appl Polym Sci 2000;77:2948;
(c) Lee D, Char K, Lee SW, Park YW. J Mater Chem 2003;13:2942.
[10] Adams PN, Devasagayam P, Pomfret SJ, Abell L, Monkman A. J Phys Condens Matter 1998;10:8293.
[11] Chan HSO, Nag SC, Ho PK. Macromolecules 1994;27:2159.
[12] Laska J, Pron A, Lefrant S. J Polym Sci A Polym Chem 1995; 33:1437.
[13] Paul Raji K, Vijayanathan Veena, Pillai CKS. Synth Met 1999;104:189.
[14] Paul RK, Pillai CKS. Synth Met 2000;27:114.
[15] Kim BH, Jung JH, Kim JW, Choi HJ, Joo J. Synth Met 2000;117:115.
[16] Ikkala O, ten Brinke G. Chem Commun 2004;19:2131.
[17] Epstein AJ, Ginder JM, Zhuo F, Woo HS, Tanner DB, Richter AF, et al. Synth Met 1987;13:63.
[18] (a) Alan GM, Huang WS. Polymer 1993;34:1833;
(b) Li XG, Kang Y, Huang MR. J Comb Chem 2006;8:670.
[19] (a) Yue J, Epstein AJ. J Am Chem Soc 1990;112:2800;
(b) Yue J, Wang ZH, Cromack KR, Epstein AJ, MacDiarmid AG. J Am Chem Soc 1991;113:2665;
(c) Cao Y, Smith P, Heeger AJ. Synth Met 1989;32:263.
[20] (a) Liu YJ, Kanatzidis MG. Inorg Chem 1993;32:2989;
(b) Kanatzidis MG, Wu CG, Marcy HO, DcGroot DC, Kannewurf CR, Kostikas A, et al. Adv Mater 1990;2:364;
(c) He H, Frost RL, Deng F, Zhu J, Wen X, Yuan P. Clays Clay Miner 2004;52:350.
[21] (a) Li XG, Lu QF, Huang MR. Chem A Eur J 2006;12:1349–59;
(b) Alan GM, Arthur JE. Synth Met 1995;69:85;
(c) Cao Y, Li S, Xue Z, Guo D. Synth Met 1986;16:305;
(d) Zheng W, Angelopolos M, Epstein AJ, MacDiarmid AG. Macromolecules 1997;30:2953;
(e) Chen SA, Lee HT. Macromolecules 1995;28:2858.

[22] Wang Y, Rubner MF. Synth Met 1992;47:255.
[23] Taka T, Laakso J, Levon K. Solid State Commun 1994;92:393.
[24] Nakajima H, Matsubayashi G. J Mater Chem 1995;5:105.
[25] Kanatzidis MG, Bissessur R, DeGroot DC, Schindler JL, Kannewurf CR. Chem Mater 1993;5:595.
[26] Singh R, Arora V, Tandon RP, Chandra S, Kumar N, Mansingh A. Polymer 1997;38:4897.
[27] Sivakumar S, Damodaran AD, Warrier KGK. Ceram Int 1995;21:85.
[28] Ikkala O, ten Brinke G. Science 2002;295:2407.
[29] Vaia RA, Teukolsky RK, Giannelis EP. Chem Mater 1994;8:1017.